The Journal of Chemical Physics

Diffusion in heterogeneous discs and spheres: New closed-form expressions for exit times and homogenization formulas

Cite as: J. Chem. Phys. **153**, 074115 (2020); https://doi.org/10.1063/5.0010810
Submitted: 16 April 2020 . Accepted: 30 July 2020 . Published Online: 21 August 2020

Elliot J. Carr, Jacob M. Ryan, and Matthew J. Simpson

AIP Publishing

The Journal of Chemical Physics ARTICLE scitation.org/journal/jcp

Diffusion in heterogeneous discs and spheres: New closed-form expressions for exit times and homogenization formulas

Cite as: J. Chem. Phys. 153, 074115 (2020); doi: 10.1063/5.0010810
Submitted: 16 April 2020 • Accepted: 30 July 2020 •
Published Online: 21 August 2020

Elliot J. Carr,[a] Jacob M. Ryan, and Matthew J. Simpson

AFFILIATIONS

School of Mathematical Sciences, Queensland University of Technology, Brisbane, Australia

[a]Author to whom correspondence should be addressed: elliot.carr@qut.edu.au

ABSTRACT

Mathematical models of diffusive transport underpin our understanding of chemical, biochemical, and biological transport phenomena. Analysis of such models often focuses on relatively simple geometries and deals with diffusion through highly idealized homogeneous media. In contrast, practical applications of diffusive transport theory inevitably involve dealing with more complicated geometries as well as dealing with heterogeneous media. One of the most fundamental properties of diffusive transport is the concept of *mean particle lifetime* or *mean exit time*, which are particular applications of the concept of *first passage time* and provide the mean time required for a diffusing particle to reach an absorbing boundary. Most formal analysis of mean particle lifetime applies to relatively simple geometries, often with homogeneous (spatially invariant) material properties. In this work, we present a general framework that provides exact mathematical insight into the mean particle lifetime, and higher moments of particle lifetime, for point particles diffusing in heterogeneous discs and spheres with radial symmetry. Our analysis applies to geometries with an arbitrary number and arrangement of distinct layers, where transport in each layer is characterized by a distinct diffusivity. We obtain exact closed-form expressions for the mean particle lifetime for a diffusing particle released at an arbitrary location, and we generalize these results to give exact, closed-form expressions for any higher-order moment of particle lifetime for a range of different boundary conditions. Finally, using these results, we construct new homogenization formulas that provide an accurate simplified description of diffusion through heterogeneous discs and spheres.

I. INTRODUCTION

Mathematical models describing diffusive transport of mass and energy are essential for our understanding of many processes in physics,[1–3] engineering,[4–6] and biology.[7,8] Analysis of mathematical models of diffusive transport primarily focuses on diffusion in relatively simple geometries and homogeneous materials.[1–6] In contrast, applications of diffusive transport theory in more complicated geometries and/or with heterogeneous materials are more often explored computationally.[9–14] While computational approaches for understanding and interpreting mathematical models of diffusive transport are necessary in certain circumstances, analytical insight is always attractive where possible because it provides simple, easy-to-evaluate, closed-form mathematical expressions that explicitly highlight key relationships.[15] Such a general insight is not always possible when relying on computational methods alone.

A fundamental property of diffusive transport is the concept of *particle lifetime*, which is a particular application of the first passage time.[1–3] Developing analytical and computational tools to characterize particle lifetime provides insight into how varying material properties and geometry affect the time taken for a diffusing particle to reach a certain target.[16–23] Many results about particle lifetime for diffusive transport have been presented, often in relatively simple homogeneous geometries[1,24,25] with certain limited extensions to cases involving more detailed geometries and specific forms of material heterogeneity.[23,26–29]

In this work, we consider diffusive transport in heterogeneous materials in two and three dimensional domains with radial symmetry. Such geometries are relevant to a number of important

applications in the biophysics literature including the study of transport phenomena in compound droplets[30,31] and the study of nutrient delivery in three-dimensional organoid culture.[32–35] Our modeling framework is very general: we consider diffusion in discs and spheres, with an arbitrary number and an arbitrary arrangement of distinct layers, where the transport in each layer is characterized by a distinct arbitrary diffusivity. In this work, we show how to obtain exact solutions for the mean particle lifetime for a diffusing particle released at an arbitrary location, and we generalize these results to give exact, closed-form expressions for any higher-order moment of particle lifetime for a range of different boundary conditions. With this information, we construct new homogenization formulas[36] that allow us to capture key particle lifetime properties in a complex heterogeneous medium with a simpler equivalent homogeneous medium. These formulas extend many previous formulas that are relevant in one dimension for relatively simple forms of heterogeneity.[23,37–41] To test the veracity of the new exact calculations, we implement a stochastic random walk model and show that the exact calculations match appropriately averaged simulation data. Matlab code to implement the random walk and Maple code to implement the exact calculations are provided on GitHub.[43]

II. RESULT AND DISCUSSION

A. Discrete model and stochastic simulations

Consider a diffusing particle in a line, disc, or sphere that is partitioned into m distinct layers, $\mathcal{L}_i = (R_{i-1}, R_i)$ for $i = 1, \ldots, m$, where $R_0 < R_1 < \cdots < R_m$ (Fig. 1). Each layer may take on a distinct diffusivity, $D_i > 0$ for $i = 1, \ldots, m$. The inner and outer boundaries are located at $r = R_0$ and $r = R_m$, respectively, and $r = R_i$ specifies the location of the interface between layers i and $i + 1$ ($i = 1, \ldots, m - 1$). Note that choosing $R_0 = 0$ means that we are considering an entire disc or sphere while choosing $R_0 > 0$ produces an annulus in two dimensions or a spherical shell in three dimensions. If $R_0 > 0$, either the inner or outer boundary is designated as the absorbing boundary with the other boundary assumed to be reflecting. Otherwise, if $R_0 = 0$, the outer boundary is designated as the absorbing boundary. We refer to the case of an absorbing outer boundary as the *outward* configuration and the case of an absorbing inner boundary as the *inward* configuration.

We now consider a random walk on the line, disc, or sphere. Here, a particle undergoes a random walk with constant steps of distance $\delta > 0$ and constant time steps of duration $\tau > 0$. When the geometry is heterogeneous, the probability of the particle moving to a new position at each time step varies across the layers with probability P_i and diffusivity $D_i = P_i\delta^2/(2d\tau)$ associated with layer i, where $d = 1, 2, 3$ is the dimension. For all geometries, the random walk continues until the particle hits the absorbing boundary, at which point the number of steps is recorded. In Secs. II A 1 and II A 2, we consider the cases of the disc and sphere only with our implementation of the random walk on a heterogeneous line presented in our previous work.[23]

1. Heterogeneous disc

Let $\mathbf{x}(t) = [x(t), y(t)]$ be the position of the particle at time t and $\mathcal{C}(\mathbf{x}(t); \delta)$ be the circle of radius δ centered at $\mathbf{x}(t)$. If $\mathcal{C}(\mathbf{x}(t); \delta)$ is located entirely within a single layer, say layer i [i.e., $\mathcal{C}(\mathbf{x}(t); \delta) \subset \mathcal{L}_i$], then the following outcomes are possible during the next time step: (i) the particle moves to position $\mathbf{x}(t + \tau) = [x(t) + \delta\cos(\theta), y(t) + \delta\sin(\theta)]$ with probability P_i, where $\theta \sim \mathcal{U}[0, 2\pi]$; (ii) the particle remains at its current position, $\mathbf{x}(t)$, with probability $1 - P_i$. If $\mathcal{C}(\mathbf{x}(t); \delta)$ intersects an interface, say $r = R_i$, then the following outcomes are possible during the next time step: (i) the particle moves to one of the n positions: $\mathbf{x}(t + \tau) = [x(t) + \delta\cos(\theta_k), y(t) + \delta\sin(\theta_k)]$ ($k = 1, \ldots, n$), where $\theta_k = 2\pi(k - 1)/n$ with probability $\mathcal{P}_k/n$; (ii) the particle remains at its current position, $\mathbf{x}(t)$, with probability $1 - \sum_{k=1}^{n} \mathcal{P}_k/n$. Here, $\mathcal{P}_k$ is the probability associated with the layer in which the position $[x(t) + (\delta/2)\cos(\theta_k), y(t) + (\delta/2)\sin(\theta_k)]$ is located. If $\mathcal{C}(\mathbf{x}(t); \delta)$ intersects the reflecting boundary, the following outcomes are possible during the next time step: (i) the particle attempts to move to position $\mathbf{x}(t + \tau) = [x(t) + \delta\cos(\theta), y(t) + \delta\sin(\theta)]$, where $\theta \sim \mathcal{U}[0, 2\pi]$ with probability $\mathcal{P}_b$; (ii) the particle remains at its current position, $\mathbf{x}(t)$, with probability $1 - \mathcal{P}_b$. Here, $\mathcal{P}_b = P_1$ for the outward configuration, and $\mathcal{P}_b = P_m$ for the inward configuration. If the potential step in (i) would require the particle to pass through the reflecting boundary, then the step is aborted.

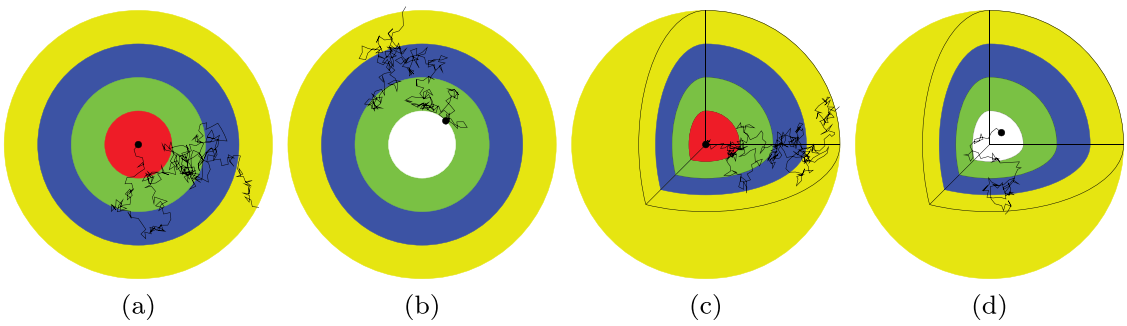

FIG. 1. Schematic of a random walk for a particle starting at the inner boundary and exiting at the outer boundary for the (a) heterogeneous disc, (b) heterogeneous annulus, (c) heterogeneous sphere, and (d) heterogeneous spherical shell. In each case, the inner and outer boundaries are at $r = R_0$ and $r = R_m$, and the location of the interface between layers i and $i + 1$ is $r = R_i$ for $i = 1, \ldots, m - 1$. In (a) and (c), $R_0 = 0$, while in (b) and (d), $R_0 > 0$. For the spheres, an octant has been removed to show the layered structure.

2. Heterogeneous sphere

Let $\mathbf{x}(t) = [x(t), y(t), z(t)]$ be the position of the particle at time t and $\mathcal{S}(\mathbf{x}(t);\delta)$ be the sphere of radius δ centered at $\mathbf{x}(t)$. If $\mathcal{S}(\mathbf{x}(t);\delta)$ is located entirely within a single layer, say layer i [i.e., $\mathcal{S}(\mathbf{x}(t);\delta) \subset \mathcal{L}_i$], then the following outcomes are possible during the next time step: (i) the particle moves to position $\mathbf{x}(t+\tau) = [x(t) + \delta\sin(\phi)\cos(\theta), y(t) + \delta\sin(\phi)\sin(\theta), z(t) + \delta\cos(\phi)]$ with probability P_i, where $\phi = \cos^{-1}(1-2u)$, $u \sim \mathcal{U}[0,1]$, and $\theta \sim \mathcal{U}[0,2\pi]$; (ii) the particle remains at its current position, $\mathbf{x}(t)$, with probability $1 - P_i$. The formula for ϕ avoids the clustering of random points around the poles ($\phi = 0$ and $\phi = \pi$) when ϕ is naively sampled from $\mathcal{U}[0,\pi]$.[42] If $\mathcal{S}(\mathbf{x}(t);\delta)$ intersects an interface, say $r = R_i$, then the following outcomes are possible during the next time step: (i) the particle moves to one of the $n = n_1 n_2$ positions: $\mathbf{x}(t+\tau) = [x(t) + \delta\sin(\phi_j)\cos(\theta_k), y(t) + \delta\sin(\phi_j)\sin(\theta_k), z(t) + \delta\cos(\phi_j)]$ ($j = 1, \ldots, n_1$, $k = 1, \ldots, n_2$) with probability $\mathcal{P}_{j,k}/n$, where $\phi_j = \cos^{-1}(1 - 2(j-1)/n_1)$ and $\theta_k = 2\pi(k-1)/n_2$; (ii) the particle remains at its current position, $\mathbf{x}(t)$, with probability $1 - \sum_{j=1}^{n_1}\sum_{k=1}^{n_2}\mathcal{P}_{j,k}/n$. Here, $\mathcal{P}_{j,k}$ is the probability associated with the layer in which the position $[x(t) + (\delta/2)\sin(\phi_j)\cos(\theta_k), y(t) + (\delta/2)\sin(\phi_j)\sin(\theta_k), z(t) + (\delta/2)\cos(\phi_j)]$ is located. If $\mathcal{S}(\mathbf{x}(t);\delta)$ intersects the reflecting boundary, the following outcomes are possible during the next time step: (i) the particle attempts to move to position $\mathbf{x}(t+\tau) = [x(t) + \delta\sin(\phi)\cos(\theta), y(t) + \delta\sin(\phi)\sin(\theta), z(t) + \delta\cos(\phi)]$ with probability $\mathcal{P}_b$, where $\phi = \cos^{-1}(1-2u)$, $u \sim \mathcal{U}[0,1]$ and $\theta \sim \mathcal{U}[0,2\pi]$; (ii) the particle remains at its current position, $\mathbf{x}(t)$, with probability $1 - \mathcal{P}_b$. Here, $\mathcal{P}_b = P_1$ for the outward configuration, and $\mathcal{P}_b = P_m$ for the inward configuration. If the potential step in (i) would require the particle to pass through the reflecting boundary, then the step is aborted.

MATLAB implementations of the random walk on the heterogeneous disc and sphere are available on GitHub,[43] and simulation results are summarized in the supplementary material. These algorithms are constructed so that we can consider diffusive transport in two or three dimensions with arbitrary choices of $R_0 < R_1 < \cdots < R_m$ and $D_i > 0$ for $i = 1, \ldots, m$. The code accommodates both the outward ($r = R_m$ absorbing) and inward ($r = R_0$ absorbing) configurations as well as allowing for the initial location of the particle to be chosen arbitrarily in the interval $[R_0, R_m]$. To provide mathematical insight into these simulations, we now consider analyzing the moments of exit time.

B. Moments of exit time

Due to the symmetries inherent in the heterogeneous disc and sphere, the exit time properties are independent of the angles θ and ϕ and depend only on the radial coordinate r. Let $\mathbb{E}(T^k; r)$ be the kth moment of exit time for a particle with starting position $x(0) = r$ (line), $\mathbf{x}(0) = [x(0), y(0)] = (r, 0)$ (disc), and $\mathbf{x}(0) = [x(0), y(0), z(0)] = (r, 0, 0)$ (sphere). Suppose for either the line, disc or sphere, that the random walk is repeated n times with the same starting location r yielding the following recorded exit times: $T_1, T_2, \ldots, T_n$. Then, the kth raw moment of exit time is estimated using the stochastic simulations via

$$\mathbb{E}(T^k; r) \approx \frac{1}{n}\sum_{j=1}^{n} T_j^k, \tag{1}$$

with equality obtained in the limit as $n \to \infty$. Using our previous arguments,[23] we confirm that the continuum representation of $\mathbb{E}(T^k; r)$ in layer i, which we denote by $M_k^{(i)}(r)$, satisfies the following system of differential equations:[1,44]

$$\frac{D_i}{r^{d-1}}\frac{\mathrm{d}}{\mathrm{d}r}\left(r^{d-1}\frac{\mathrm{d}M_k^{(i)}}{\mathrm{d}r}\right) = -kM_{k-1}^{(i)}, \tag{2}$$

for $i = 1, \ldots, m$ where $r \in (R_{i-1}, R_i)$ and $d = 1, 2, 3$ is the dimension. The appropriate internal boundary conditions at the interfaces are

$$M_k^{(i-1)}(R_i) = M_k^{(i)}(R_i), \tag{3}$$

$$D_{i-1}\frac{\mathrm{d}M_k^{(i-1)}}{\mathrm{d}r}(R_i) = D_i\frac{\mathrm{d}M_k^{(i)}}{\mathrm{d}r}(R_i), \tag{4}$$

for $i = 1, \ldots, m-1$. These equations must also be supplemented with boundary conditions at $r = R_0$ and $r = R_m$. The appropriate conditions are $\mathrm{d}M_k^{(1)}(R_0)/\mathrm{d}r = 0$ and $M_k^{(m)}(R_m) = 0$ for the outward configuration and $M_k^{(1)}(R_0) = 0$ and $\mathrm{d}M_k^{(m)}(R_m)/\mathrm{d}r = 0$ for the inward configuration. For the disc and sphere, if $R_0 = 0$, then the inner boundary vanishes and a symmetry condition is imposed, $\mathrm{d}M_k^{(1)}(0)/\mathrm{d}r = 0$. The boundary value problem for $M_k^{(i)}$ for $i = 1, \ldots, m$ is solved sequentially for $k = 1, 2, \ldots$ given $M_0^{(i)}(r) = 1$ for all $r \in (R_{i-1}, R_i)$ and $i = 1, \ldots, m$, which is evident from (1) when $k = 0$.

The attraction of working with the moments of exit time is that the system of boundary value problems can be solved exactly to obtain closed-form analytical expressions for the moments in each layer in terms of the diffusivities $D_1, \ldots, D_m$ and radii $R_0, \ldots, R_m$. This can be achieved using standard symbolic software. A Maple worksheet that is capable of solving these boundary value problems is available on GitHub,[43] and a comparison between appropriately averaged data from the stochastic simulation algorithm and the solution of the relevant boundary value problems that confirm the accuracy of the expressions for the moments of exit time are detailed in the supplementary material.

A summary of closed-form expressions is provided in Table I for the outward configuration and the case where $R_0 = 0$. The first three rows in Table I show the first three moments for an homogeneous medium ($m = 1$), and we see that the algebraic expressions become increasingly complicated as we consider higher moments. The fourth row in Table I shows simple expressions for the first moment of exit time in a two-layer problem. Experimentation with Maple enables us to propose a more general expression for the first moment of exit time in a more general scenario with m layers, as shown in the fifth row of Table I. While it is possible to use the Maple worksheet provided to find values of an arbitrary moment of exit time in a problem with an arbitrary number of layers, it is much more difficult to give closed-form expressions for such higher moments.

All expressions in Table I are for discs and spheres with $R_0 = 0$ under the outward configuration. Additional results in Tables II and III compare moments of exit time formulas for an annulus and spherical shell ($R_0 > 0$) under both the outward and inward configurations. Here, we see a key difference between the results for one dimension with the results in higher dimensions. For example,

TABLE I. Moments of exit time formulas for homogeneous (m = 1) and heterogeneous (m > 1) discs and spheres with R_0 = 0 under the outward configuration. For the homogeneous case, we drop the layer index on the moments appearing in the superscript.

Homogeneous disc	Homogeneous sphere
$M_1(r) = \frac{R_1^2 - r^2}{4D_1}$ $M_2(r) = \frac{R_1^2 - r^2}{32D_1^2}\left(3R_1^2 - r^2\right)$ $M_3(r) = \frac{R_1^2 - r^2}{384D_1^3}\left(19R_1^4 - 8R_1^2r^2 + r^4\right)$	$M_1(r) = \frac{R_1^2 - r^2}{6D_1}$ $M_2(r) = \frac{R_1^2 - r^2}{180D_1^2}\left(7R_1^2 - 3r^2\right)$ $M_3(r) = \frac{R_1^2 - r^2}{2520D_1^3}\left(31R_1^4 - 18R_1^2r^2 + 3r^4\right)$
Heterogeneous disc (2 layers)	Heterogeneous sphere (2 layers)
$M_1^{(1)}(r) = \frac{R_1^2 - r^2}{4D_1} + \frac{R_2^2 - R_1^2}{4D_2}$ $M_1^{(2)}(r) = \frac{R_2^2 - r^2}{4D_2}$	$M_1^{(1)}(r) = \frac{R_1^2 - r^2}{6D_1} + \frac{R_2^2 - R_1^2}{6D_2}$ $M_1^{(2)}(r) = \frac{R_2^2 - r^2}{6D_2}$
Heterogeneous disc (m layers)	Heterogeneous sphere (m layers)
$M_1^{(i)}(r) = \frac{R_i^2 - r^2}{4D_i} + \sum_{j=i+1}^{m} \frac{R_j^2 - R_{j-1}^2}{4D_j}$, $i = 1, \ldots, m$.	$M_1^{(i)}(r) = \frac{R_i^2 - r^2}{6D_i} + \sum_{j=i+1}^{m} \frac{R_j^2 - R_{j-1}^2}{6D_j}$, $i = 1, \ldots, m$.

consider the simplest possible case of a random walk on a finite line (d = 1) in a homogeneous environment. If a diffusing particle is released in the center of the domain, the expected time to reach either boundary is equal.[1,3] In contrast, if we have a random walk in a radially symmetric homogeneous disc or sphere and a particle is released at the center of the domain, the diffusing particle takes different amounts of time to reach the two boundaries owing to the radial geometry. Such differences can be even more nuanced

TABLE II. Moments of exit time formulas for a homogeneous (m = 1) or heterogeneous (m > 1) annulus (R_0 > 0) under the inward or outward configuration. For the homogeneous case, we drop the layer index on the moments appearing in the superscript.

Homogeneous disc (outward configuration)
$M_1(r) = \frac{R_1^2 - r^2}{4D_1} + \frac{R_0^2}{2D_1}\ln\left(\frac{r}{R_1}\right)$ $M_2(r) = \frac{R_0^2}{32D_1^2}\left[8\left(r^2 + \frac{3R_0^2}{2} - R_1^2\right)\ln\left(\frac{R_1}{r}\right) + 16R_0^2\left(\ln(R_1)^2 + \ln(R_0)\ln(r) - \ln(R_0 r)\ln(R_1)\right)\right] + \frac{R_1^2 - r^2}{32D_1^2}\left(3R_1^2 - r^2 - 8R_0^2\right)$
Homogeneous disc (inward configuration)
$M_1(r) = \frac{R_0^2 - r^2}{4D_1} + \frac{R_1^2}{2D_1}\ln\left(\frac{r}{R_0}\right)$ $M_2(r) = \frac{R_1^2}{32D_1^2}\left[8\left(r^2 + \frac{3R_1^2}{2} - R_0^2\right)\ln\left(\frac{R_0}{r}\right) + 16R_1^2\left(\ln(R_0)^2 + \ln(R_1)\ln(r) - \ln(R_1 r)\ln(R_0)\right)\right] + \frac{R_0^2 - r^2}{32D_1^2}\left(3R_0^2 - r^2 - 8R_1^2\right)$
Heterogeneous disc (m layers, outward configuration)
$M_1^{(i)}(r) = \frac{R_i^2 - r^2}{4D_i} + \frac{R_0^2}{2D_i}\ln\left(\frac{r}{R_i}\right) + \sum_{j=i+1}^{m}\frac{R_j^2 - R_{j-1}^2}{4D_j} + \frac{R_0^2}{2D_j}\ln\left(\frac{R_{j-1}}{R_j}\right)$, $i = 1, \ldots, m$.
Heterogeneous disc (m layers, inward configuration)
$M_1^{(i)}(r) = \frac{R_{i-1}^2 - r^2}{4D_i} + \frac{R_m^2}{2D_i}\ln\left(\frac{r}{R_{i-1}}\right) + \sum_{j=1}^{i-1}\frac{R_{j-1}^2 - R_j^2}{4D_j} + \frac{R_m^2}{2D_j}\ln\left(\frac{R_j}{R_{j-1}}\right)$, $i = 1, \ldots, m$.

TABLE III. Moments of exit time formulas for a homogeneous ($m = 1$) or heterogeneous ($m > 1$) spherical shell ($R_0 > 0$) under the inward or outward configuration. For the homogeneous case, we drop the layer index on the moments appearing in the superscript.

Homogeneous sphere (outward configuration)
$M_1(r) = \frac{R_1^2 - r^2}{6D_1} + \frac{R_0^3}{3D_1}\left(\frac{1}{R_1} - \frac{1}{r}\right)$
$M_2(r) = \frac{R_1^2 - r^2}{180D_1^2}\left(7R_1^2 - 3r^2\right) + \frac{R_0^3}{D_1^2}\left[\frac{1}{9}\left(3r - R_1 - \frac{R_1^2}{r} - \frac{r^2}{R_1}\right) + \frac{2R_0^2}{5}\left(\frac{1}{r} - \frac{1}{R_1}\right) + \frac{2R_0^3}{9R_1}\left(\frac{1}{R_1} - \frac{1}{r}\right)\right]$
Homogeneous sphere (inward configuration)
$M_1(r) = \frac{R_0^2 - r^2}{6D_1} + \frac{R_1^3}{3D_1}\left(\frac{1}{R_0} - \frac{1}{r}\right)$
$M_2(r) = \frac{R_0^2 - r^2}{180D_1^2}\left(7R_0^2 - 3r^2\right) + \frac{R_1^3}{D_1^2}\left[\frac{1}{9}\left(3r - R_0 - \frac{R_0^2}{r} - \frac{r^2}{R_0}\right) + \frac{2R_1^2}{5}\left(\frac{1}{r} - \frac{1}{R_0}\right) + \frac{2R_1^3}{9R_0}\left(\frac{1}{R_0} - \frac{1}{r}\right)\right]$
Heterogeneous sphere (m layers, outward configuration)
$M_1^{(i)}(r) = \frac{R_i^2 - r^2}{6D_i} + \frac{R_0^3}{3D_i}\left[\frac{1}{R_i} - \frac{1}{r}\right] + \sum_{j=i+1}^{m} \frac{R_j^2 - R_{j-1}^2}{6D_j} + \frac{R_0^3}{3D_j}\left[\frac{1}{R_j} - \frac{1}{R_{j-1}}\right], \quad i = 1, \ldots, m.$
Heterogeneous sphere (m layers, inward configuration)
$M_1^{(i)}(r) = \frac{R_{i-1}^2 - r^2}{6D_i} + \frac{R_m^3}{3D_i}\left[\frac{1}{R_{i-1}} - \frac{1}{r}\right] + \sum_{j=1}^{i-1} \frac{R_{j-1}^2 - R_j^2}{6D_j} + \frac{R_m^3}{3D_j}\left[\frac{1}{R_{j-1}} - \frac{1}{R_j}\right], \quad i = 1, \ldots, m.$

when the domain is heterogeneous, and such considerations can have practical implications. For example, consider the case where we treat a biological cell as a two-layer compound sphere ($m = 2$), with the outer layer ($R_1 < r < R_2$) representing the cytoplasm and the inner layer ($0 < r < R_1$) representing the nucleus. In this case, it is of interest to estimate the expected time taken for a molecule released at the outer surface ($r = R_2$) to be absorbed at the nuclear membrane ($r = R_1$). Alternatively, it is also of interest to estimate the expected time taken for a protein synthesized in the nucleus to diffuse from the nuclear membrane ($r = R_1$) to the exterior cell membrane ($r = R_2$). These effects of directionality are explicitly described in the formulas in Tables II and III.

Vaccario *et al.*[29] present closed-form expressions for the first moment of exit time for lines, discs, and spheres with $R_0 > 0$ derived using a stochastic differential equation description of the random walk process. The results are given for two layers under the inward configuration and depend on the convention of the stochastic integral (Itô, Stratonovich, or isothermal). Interestingly, our closed-form expressions for the first moment of exit time in Table III match those reported by Vaccario *et al.* for the isothermal convention. As reported in the supplementary material, the solution of the continuum description (2)–(4) matches with appropriately averaged data from our discrete stochastic model, which includes an assumption specifying how the random walk interacts with the interfaces at $r = R_i$ for $i = 1, \ldots, m - 1$ (see Secs. II A 1 and II A 2). We acknowledge that a different assumption at the interface would likely lead to a different continuum description. Nonetheless, we focus here on this particular implementation since our assumptions about the jump probabilities at the interface are minimal and provide a straightforward means of incorporating spatial variations in diffusivity.

Figure 2 compares the spatial distribution of the first moment of exit times for a range of problems in heterogeneous lines, discs, and spheres with two layers ($m = 2$). Profiles in Fig. 2(a) show the first moment for a problem with $50 < r < 150$ with an interface at the midpoint, $r = 100$. The results for the outward configuration show that the spatial distribution of the first moment is relatively sensitive to the dimension of the problem since we observe distinct results for $d = 1, 2, 3$. Similarly, the results for the inward configuration indicate that the spatial distribution of the first moment is also relatively sensitive to the dimensionality. The results in Fig. 2(a) demonstrate that for the inward configuration, the first moment of exit time is largest for the sphere and smallest for the line, while the opposite is true for the outward configuration. For example, the mean time for a particle released at the outer boundary to exit at the inner boundary for the problem in Fig. 2(a) is 2.3×10^5, 3.6×10^5, and 6.1×10^5 for the line, disc, and sphere, respectively. On the other hand, the mean time for a particle released at the inner boundary to exit at the outer boundary is 9.8×10^4, 7.6×10^4, and 6.2×10^4 for the line, disc, and sphere, respectively. These differences can be explained by the geometry-induced outward bias inherent in the random walk on the disc and the sphere, where a particle is more likely to move away from the origin in the positive r direction due to the circular and spherical geometries. This geometry-induced outward bias is absent

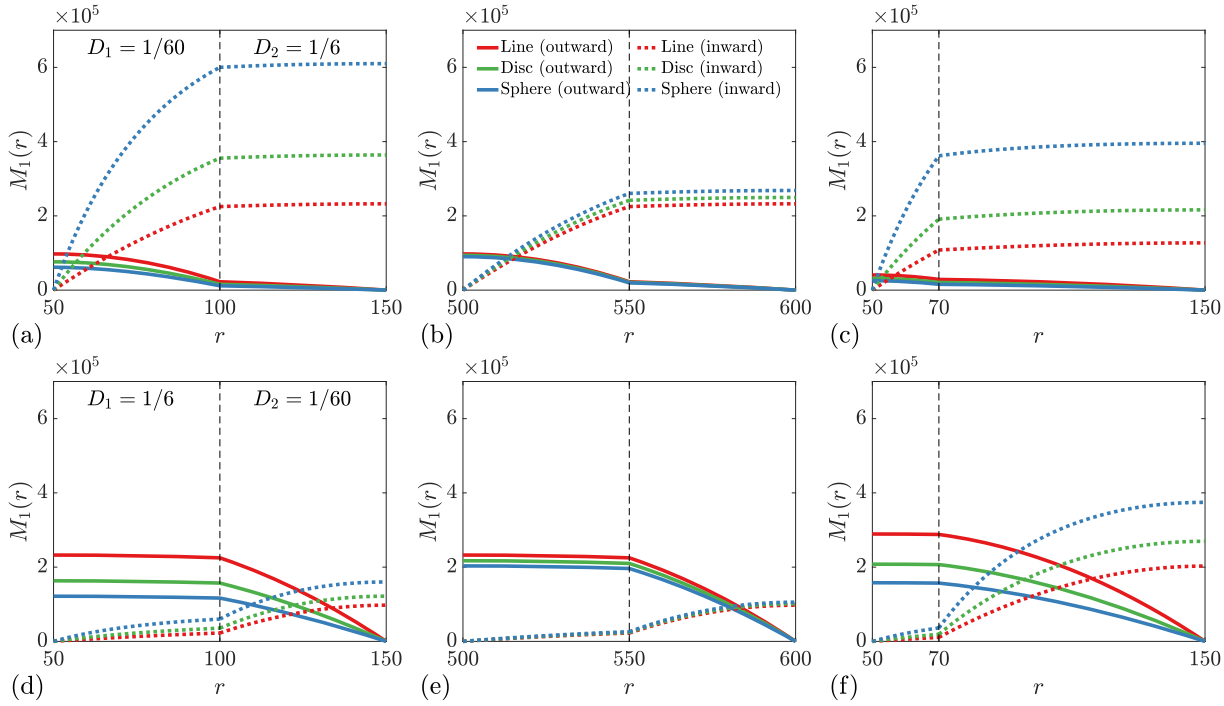

FIG. 2. First moment of exit time $M_1(r)$ for a range of cases in heterogeneous discs and spheres with two layers. Each figure compares random walks on lines (d = 1, red), discs (d = 2, green), and spheres (d = 3, blue) for both the outward (solid) and inward (dashed) configurations. For (a)–(c), we have D_1 = 1/60 and D_2 = 1/6, while for (d)–(f), we have D_1 = 1/6 and D_2 = 1/60. Cases in (a), (c), (d), and (f) correspond to R_0 = 50 and R_2 = 150, while cases in (b) and (e) correspond to R_0 = 500 and R_2 = 600. The legend in (b) applies to all figures.

on the line, which explains why the mean exit time on a line is smallest for the inward configuration and largest for the outward configuration [see Fig. 2(a)].

The results in Fig. 2(b) show the spatial distribution of the first moment for a similar problem with $500 < r < 600$ with an interface at the midpoint, $r = 550$. Therefore, the dimensions of the problem in Fig. 2(b) are very similar to those in Fig. 2(a) except the effects of the geometry are more pronounced in Fig. 2(a) since the domain is closer to the origin. As a result, the profiles for the first moment in Fig. 2(b) are much less sensitive to position than those in Fig. 2(a) since the geometric differences between $d = 1$, 2 and $d = 3$ are far less pronounced when r is larger. This is explained by the geometry-induced outward bias present for the disc and sphere, which is proportional to $(d - 1)/r$ and therefore more dominant when the domain is closer to the origin. This observation also explains why the spatial distributions of the first moment of exit time for the disc and sphere approach the spatial distributions of the first moment of exit time for the line in Fig. 2(b) since the domain $500 < r < 600$ is far from the origin. For the outward configuration, the spatial distributions of the first moment of exit time for the disc and sphere increase from Fig. 2(a) to Fig. 2(b) since a particle is less likely to move outward for the problem in Fig. 2(b) than for the problem in Fig. 2(a). Similarly, for the inward configuration, the first moment of exit time for the disc and sphere decreases since a particle is more likely to move inward for the problem in Fig. 2(b) than for the problem in Fig. 2(a). The spatial distributions of the first moment of exit time for the line in Fig. 2(b) remain unchanged from Fig. 2(a) as there is no geometry-induced outward bias for the random walk on the line.

Profiles in Fig. 2(c) show the first moment for a problem with $50 < r < 150$ with an interface at $r = 70$. Therefore, the only difference between the problems in Figs. 2(a) and 2(c) is the location of the interface, and here, we see that when the interface is at $r = 70$, the dependence on d is much less pronounced for the outward configuration, whereas the dependence on d is much more pronounced for the inward configuration. For the inward configuration in Fig. 2(c), a particle released in the second layer is required to pass through a thinner layer of the lower diffusivity material to exit at $r = 50$ compared to Fig. 2(a). This explains the results in Figs. 2(a) and 2(c) for the inward configuration, where we see that the mean exit time remains largely unchanged for $50 < r < 70$ but reduces significantly for $70 < r < 150$.

The results in Figs. 2(d)–2(f) show the spatial distribution of the first moment when the values of D_1 and D_2 for the problems in Figs. 2(a)–2(c) are interchanged. Comparing the results for the inward configuration in Figs. 2(a) and 2(b) with the results for the outward configuration in Figs. 2(d) and 2(e), we see that the profiles for the line are symmetrical to each other about the interface. As there is no geometry-induced outward bias on the line and the interface is located at the midpoint of the domain, the outward

configuration in Figs. 2(a) and 2(b) is equivalent to the inward configuration in Figs. 2(d) and 2(e) leading to the observed symmetry. Another observation evident from Figs. 2(d)–2(f) is that the first moment of exit time is approximately uniform in the first layer for the outward configuration. This is because D_1 is an order of magnitude greater than D_2. Thus, the exit time for a particle released in the first layer is dominated by the time taken for the particle to pass through the second layer. A similar argument explains the approximately uniform mean exit time distribution in the second layer for the inward configuration in Figs. 2(a)–2(c).

The key trends in the distribution of the first moment profiles in Figs. 2(a)–2(f) are echoed in the trends in the second and higher moment profiles (not shown). Now that we have constructed, validated, and explored exact solutions for arbitrary moments of exit time for diffusion in a wide range of heterogeneous discs and spheres, we can use these results to derive new homogenization formulas.

C. Homogenization results

We now consider the problem of approximating a stochastic random walk on a heterogeneous disc or sphere with a stochastic random walk on an equivalent or *effective* homogeneous disc or sphere. Here, we assume that the homogenized stochastic model takes the form of an unbiased random walk with diffusivity D_{eff} and probability $P_{\text{eff}} = 2d\tau D_{\text{eff}}/\delta^2$. To keep the derivation succinct, we consider the case where the particles are released at the reflecting boundary ($r = R_0$ for the outward configuration and $r = R_m$ for the inward configuration). We choose D_{eff} to constrain the first moment of exit time for the homogenized random walk to be equal to the first moment of exit time for the heterogeneous random walk at the starting position of the particle, that is, $M_1^{\text{eff}}(R_0) = M_1^{(1)}(R_0)$ for the outward configuration and $M_1^{\text{eff}}(R_m) = M_1^{(m)}(R_m)$ for the inward configuration. Combining these constraints with the closed-form expressions for the moments of exit time in Tables I–III [note: $M_1^{\text{eff}}(r)$ denotes $M_1(r)$ with $D_1 = D_{\text{eff}}$ and $R_1 = R_m$] and rearranging for D_{eff} yield simple closed-form formulas for the effective diffusivity listed in Table IV. Identifying the pattern in these homogenization formulas and the corresponding formulas for the heterogeneous line,[23] we identify the general homogenization formula given in Table IV, which is valid for all three dimensions ($d = 1, 2, 3$), and both the inward and outward configurations for the case when a particle is released at the reflecting boundary.

We now provide a visual interpretation of the homogenization approximation for heterogeneous discs and spheres in Fig. 3. The results in this figure are generated by considering a random walk with $\delta = \tau = 1$ in a heterogeneous disc [Fig. 3(a)] and a heterogeneous sphere [Fig. 3(b)] consisting of two layers ($m = 2$) with

TABLE IV. Effective diffusivity formulaS for a heterogeneous ($m > 1$) annulus or spherical shell ($R_0 > 0$) under the inward or outward configuration for a particle released at the reflecting boundary ($r = R_0$ for the outward configuration and $r = R_m$ for the inward configuration).

Heterogeneous disc (m layers, outward configuration)
$D_{\text{eff}} = \left[\frac{R_m^2 - R_0^2}{4} + \frac{R_0^2}{2}\ln\left(\frac{R_0}{R_m}\right)\right] \Big/ \left[\sum_{j=1}^{m} \frac{R_j^2 - R_{j-1}^2}{4D_j} + \frac{R_0^2}{2D_j}\ln\left(\frac{R_{j-1}}{R_j}\right)\right]$
Heterogeneous disc (m layers, inward configuration)
$D_{\text{eff}} = \left[\frac{R_m^2 - R_0^2}{4} + \frac{R_m^2}{2}\ln\left(\frac{R_0}{R_m}\right)\right] \Big/ \left[\sum_{j=1}^{m} \frac{R_j^2 - R_{j-1}^2}{4D_j} + \frac{R_m^2}{2D_j}\ln\left(\frac{R_{j-1}}{R_j}\right)\right]$
Heterogeneous sphere (m layers, outward configuration)
$D_{\text{eff}} = \left[\frac{R_m^2 - R_0^2}{6} + \frac{R_0^3}{3}\left(\frac{1}{R_m} - \frac{1}{R_0}\right)\right] \Big/ \left[\sum_{j=1}^{m} \frac{R_j^2 - R_{j-1}^2}{6D_j} + \frac{R_0^3}{3D_j}\left(\frac{1}{R_j} - \frac{1}{R_{j-1}}\right)\right]$
Heterogeneous sphere (m layers, inward configuration)
$D_{\text{eff}} = \left[\frac{R_m^2 - R_0^2}{6} + \frac{R_m^3}{3}\left(\frac{1}{R_m} - \frac{1}{R_0}\right)\right] \Big/ \left[\sum_{j=1}^{m} \frac{R_j^2 - R_{j-1}^2}{6D_j} + \frac{R_m^3}{3D_j}\left(\frac{1}{R_j} - \frac{1}{R_{j-1}}\right)\right]$
Heterogeneous line ($d = 1$), disc ($d = 2$) or sphere ($d = 3$) (m layers)
$D_{\text{eff}} = \left[\frac{R_m^2 - R_0^2}{2d} - \frac{\widetilde{R}^d}{d}\int_{R_0}^{R_m} \frac{1}{r^{d-1}}\,\mathrm{d}r\right] \Big/ \left[\sum_{j=1}^{m} \frac{R_j^2 - R_{j-1}^2}{2dD_j} - \frac{\widetilde{R}^d}{dD_j}\int_{R_{j-1}}^{R_j} \frac{1}{r^{d-1}}\,\mathrm{d}r\right]$ where $\widetilde{R} = R_0$ (outward) or $\widetilde{R} = R_m$ (inward).

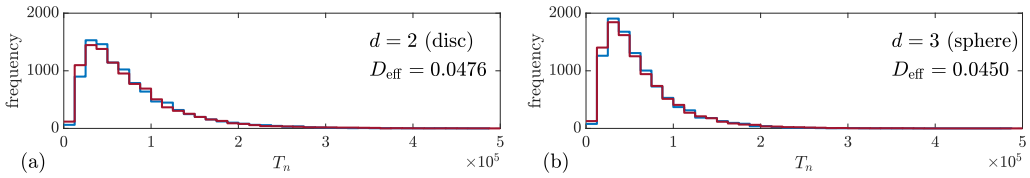

FIG. 3. Histograms of 10 000 realizations of a two-layer heterogeneous random walk (thick blue) and an effective homogeneous random walk (thin red). The two-layer random walk is described by $D_1 = 1/60$, $D_2 = 1/6$, $R_0 = 50$, $R_1 = 100$, and $R_2 = 150$. The effective homogeneous random walk is described using the same geometry but with $D_1 = D_2 = D_{\text{eff}}$ from Table IV. Both random walks assume an outward configuration and $\delta = \tau = 1$. The results in (a) correspond to $n = 24$, and those in (b) correspond to $n_1 = n_2 = 12$ (see Secs. II A 1 and II A 2).

$R_0 = 50$, $R_2 = 150$, and the interface at the center, $R_1 = 100$. We consider an order-of-magnitude difference in the diffusivities in the two media so that we demonstrate the performance of the new homogenization formulas for relatively strong heterogeneity.[23] For both the disc and the sphere, we consider 10 000 identically prepared outward-configuration simulations with a particle placed at $r = R_0$ and simulations performed until the particle reaches the absorbing boundary at $r = R_2$. In each simulation, we record the exit time, T_n, for $n = 1, \ldots, 10\,000$, and we construct a histogram of the particle lifetime as given in Fig. 3.

To generate the effective homogenized random walk results in Fig. 3, we simulate using the same geometry and boundary conditions as in the heterogeneous case but with $D_1 = D_2 = D_{\text{eff}}$, where D_{eff} is computed from the outward configuration formulas in Table IV. Performing 10 000 identically prepared realizations of the simpler homogeneous random walks, again with $\delta = \tau = 1$, we record the exit time and superimpose the histogram of the exit time distribution on the results for the true heterogeneous problem in Fig. 3 where we see that the histograms for the effective homogenized disc and sphere are very similar to those of the true heterogeneous disc and sphere. Additional results for the inward configuration or different arrangements of heterogeneous layers give rise to similar results (not shown).

III. CONCLUSION

In this work, we consider random walk models of diffusion in heterogeneous environments with the aim of constructing, and validating, new exact formulas for exit time properties and homogenization. Most exact results in the literature correspond to problems in relatively simple geometries with homogeneous material properties.[1,24,25] Some consideration has been given to certain cases of heterogeneity.[23,27–29] For example, Vaccario and colleagues[29] present exact expressions for the mean first passage time for a point particle diffusing in a spherically symmetric d-dimensional heterogeneous domains. However, this previous study was limited to just two layers with one particular arrangement of boundary conditions. In contrast, our approach deals with an arbitrary number of layers, each layer of arbitrary thickness and each layer with a distinct arbitrary value of the diffusivity. Our approach is very flexible since we provide a framework that enables us to calculate exact expressions for any moment of the distribution of exit time, and symbolic software is provided on GitHub[43] to facilitate such computations. With such exact expressions, we calculate a new suite of homogenization results that allow us to approximate some particular heterogeneous system with an effective homogeneous system with diffusivity D_{eff}.

There are many possible extensions of the work presented here. For example, the homogenization formulas in Table IV are based on approximating a heterogeneous problem with an effective homogeneous media such that the first moment of exit time in the homogenized problem is identical to the first moment of exit time in the heterogeneous problems. There are other ways that one could define an effective medium. For example, another approach is to constrain D_{eff} in such a way that the homogenized system also accounts for higher moments of the exit time distribution.[23] Another extension would be to consider the exit time distributions for growing lines, discs, and spheres that has been considered previously in the case of diffusion through homogeneous materials,[15,45] but not through heterogeneous materials.

SUPPLEMENTARY MATERIAL

See the supplementary material for additional computational results that confirm the accuracy of the moment expressions derived in Sec. II B.

ACKNOWLEDGMENTS

This work was supported by the Australian Research Council (Grant No. DP200100177). We thank the anonymous reviewer for their helpful comments that improved the quality of the final manuscript.

DATA AVAILABILITY

The data that support the findings of this study are openly available in GitHub at https://github.com/elliotcarr/Carr2020c.

REFERENCES

[1] S. Redner, *A Guide to First Passage Processes* (Cambridge University Press, 2001).
[2] P. L. Krapivsky, S. Redner, and E. Ben-Naim, *A Kinetic View of Statistical Physics* (Cambridge University Press, 2010).
[3] B. D. Hughes, *Random Walks in Random Environments* (Oxford University Press, 1995).
[4] J. Bear, *Dynamics of Fluids in Porous Media* (Elsevier, 1971).
[5] J. Crank, *The Mathematics of Diffusion* (Oxford University Press, 1975).

[6]R. B. Bird, W. R. Stewart, and E. N. Lightfoot, *Transport Phenomena* (John Wiley and Sons, 2002).
[7]J. D. Murray, *Mathematical Biology: I. An Introduction* (Springer, 2002).
[8]E. A. Codling, M. J. Plank, and S. Benhamou, "Random walk models in biology," J. R. Soc., Interface **5**, 813–834 (2008).
[9]E. S. Oran and J. P. Boris, *Numerical Simulation of Reactive Flow* (Cambridge University Press, 2001).
[10]M. J. Saxton, "Anomalous diffusion due to obstacles: A Monte Carlo study," J. Chem. Phys. **66**, 394–401 (1994).
[11]D. Lepzelter and M. Zaman, "Subdiffusion of proteins and oligomers on membranes," J. Chem. Phys. **137**, 175102 (2012).
[12]A. J. Ellery, M. J. Simpson, S. W. McCue, and R. E. Baker, "Characterizing transport through a crowded environment with different obstacle sizes," J. Chem. Phys. **140**, 054108 (2014).
[13]A. J. Ellery, R. E. Baker, and M. J. Simpson, "Distinguishing between short-time non-Fickian diffusion and long-time Fickian diffusion for a random walk on a crowded lattice," J. Chem. Phys. **144**, 171104 (2016).
[14]M. J. Simpson, "Calculating groundwater response times for flow in heterogeneous porous media," Groundwater **56**, 337–342 (2018).
[15]M. J. Simpson and R. E. Baker, "Exact calculations of survival probability for diffusion on growing lines, disks and spheres: The role of dimension," J. Chem. Phys. **143**, 094109 (2015).
[16]P. Lötstedt and L. Meinecke, "Simulation of stochastic diffusion via first exit times," J. Comput. Phys. **300**, 862–886 (2015).
[17]L. Meinecke, S. Engblom, A. Hellander, and P. Lötstedt, "Analysis and design of jump coefficient in discrete stochastic diffusion models," SIAM J. Sci. Comput. **38**, A55–A83 (2016).
[18]L. Meinecke and P. Lötstedt, "Stochastic diffusion processes on Cartesian meshes," J. Comput. Appl. Math. **294**, 1–11 (2016).
[19]L. Meinecke, "Multiscale modeling of diffusion in a crowded environment," Bull. Math. Biol. **79**, 2672–2695 (2017).
[20]A. M. Berezhkovskii, C. Sample, and S. Y. Shvartsman, "How long does it take to establish a morphogen gradient?," Biophys. J. **99**, L59–L61 (2010).
[21]A. M. Berezhkovskii and S. Y. Shvartsman, "Physical interpretation of mean local accumulation time of morphogen gradient formation," J. Chem. Phys. **135**, 154115 (2011).
[22]E. J. Carr and M. J. Simpson, "Rapid calculation of maximum particle lifetime for diffusion in complex geometries," J. Chem. Phys. **148**, 094113 (2018).
[23]E. J. Carr and M. J. Simpson, "New homogenization approaches for stochastic transport through heterogeneous media," J. Chem. Phys. **150**, 044104 (2019).
[24]A. J. Ellery, M. J. Simpson, S. W. McCue, and R. E. Baker, "Critical timescales for advection–diffusion–reaction processes," Phys. Rev. E **85**, 041135 (2012).
[25]A. J. Ellery, M. J. Simpson, S. W. McCue, and R. E. Baker, "Moments of action provide insight into critical times for advection-diffusion-reaction processes," Phys. Rev. E **86**, 031136 (2012).
[26]E. J. Carr, "Characteristic time scales for diffusion processes through layers and across interfaces," Phys. Rev. E **97**, 042115 (2018).
[27]V. Kurella, J. C. Tzou, D. Coombs, and M. J. Ward, "Asymptotic analysis of first passage time problems inspired by ecology," Bull. Math. Biol. **77**, 83–125 (2014).
[28]A. E. Lindsay, T. Kolokolnikov, and J. C. Tzou, "Narrow escape problem with a mixed trap and the effect of orientation," Phys. Rev. E **91**, 032111 (2015).
[29]G. Vaccario, C. Antoine, and J. Talbot, "First-passage times in d-dimensional heterogeneous media," Phys. Rev. Lett. **115**, 240601 (2015).
[30]K. A. Landman, "On the crenation of a compound liquid droplet," Stud. Appl. Math. **69**, 51–63 (1983).
[31]K. A. Landman, "Stability of a viscous compound fluid drop," AIChE J. **31**, 567–573 (1985).
[32]M. Ma, A. Chiu, G. Sahay, J. C. Doloff, N. Dholakia, R. Thakrar, J. Cohen, A. Vegas, D. Chen, K. M. Bratlie, T. Dang, R. L. York, J. Hollister-Lock, G. C. Weir, and D. G. Anderson, "Core-shell hydrogel microcapsules for improved islets encapsulation," Adv. Healthcare Mater. **2**, 667–672 (2013).
[33]C. C. King, A. A. Brown, I. Sargin, K. M. Bratlie, and S. P. Beckman, "Modeling of reaction-diffusion transport into a core-shell geometry," J. Theor. Biol. **460**, 204–208 (2019).
[34]M. J. Simpson and A. J. Ellery, "An analytical solution for diffusion and nonlinear uptake of oxygen in a spherical cell," Appl. Math. Modell. **36**, 3329–3334 (2012).
[35]J. A. Leedale, J. A. Kyffin, A. L. Harding, H. E. Colley, C. Murdoch, P. Sharma, D. P. Williams, S. D. Webb, and R. N. Bearon, "Multiscale modelling of drug transport and metabolism in liver spheroids," Interface Focus **10**, 20190041 (2019).
[36]Y. Davit, C. G. Bell, H. M. Byrne, A. C. Lloyd, A. C. Chapman, L. S. Kimpton, G. E. Lang, K. H. L. Leonard, J. M. Oliver, N. C. Pearson, R. J. Shipley, S. L. Waters, J. P. Whiteley, B. D. Wood, and M. Quintard, "Homogenization via formal multiscale asymptotics and volume averaging: How do the two techniques compare?," Adv. Water Resour. **62**, 178–206 (2013).
[37]B. Derrida, "Velocity and diffusion constant of a periodic one-dimensional hopping model," J. Stat. Phys. **31**, 433–450 (1982).
[38]A. M. Berezhkovskii, V. Y. Zitserman, and S. Y. Shvartsman, "Effective diffusivity in periodic porous materials," J. Chem. Phys. **119**, 6991–6993 (2003).
[39]J. R. Kalnin and A. M. Berezhkovskii, "Note: On the relation between Lifson-Jackson and Derrida formulas for effective diffusion coefficient," J. Chem. Phys. **139**, 196101 (2013).
[40]J. R. Kalnin and E. A. Kotomin, "The effective diffusion coefficient in a one-dimensional discrete lattice with the inclusions," Physica B **470-471**, 50–52 (2015).
[41]M. Huysmans and A. Dassargues, "Equivalent diffusion coefficient and equivalent diffusion accessible porosity of a stratified porous medium," Transp. Porous Media **66**, 421–438 (2007).
[42]E. W. Weisstein, Sphere point picking. MathWorld—A Wolfram web resource, https://mathworld.wolfram.com/SpherePointPicking.html, 2019.
[43]E. J. Carr, J. M. Ryan, and M. J. Simpson, https://github.com/elliotcarr/Carr2020c, 2020.
[44]S. Karlin and H. M. Taylor, *A Second Course in Stochastic Processes* (Academic Press, 1981).
[45]M. J. Simpson, J. A. Sharp, and R. E. Baker, "Survival probability for a diffusive process on a growing domain," Phys. Rev. E **91**, 042701 (2015).